Deposition of TiO_2/Ni/CuO/ITO Multi-layered Cell for Solar-driven Water Splitting

Kee-Rong Wu[1, *], Chung-Hsuang Hung[**], Chung-Wei Yeh[***], Sin-Han Fang[****]

[*] National Kaohsiung Marine University, krwu@mail.nkmu.edu.tw
[**] National Kaohsiung First University of Science and Technology, jeremyh@ccms.nkfust.edu.tw
[***] Kao Yuan University, Kaohsiung, Taiwan, t90026@cc.kyu.edu.tw
[****] National Kaohsiung Marine University, rice77720@gmail.com

ABSTRACT

A photoelectrolysis cell based on multilayered TiO_2/Ni/CuO/ITO (M-cell) photoelectrode is prepared on ITO substrate using a multi-target magnetron sputtering technique in which Ni acts as an ohmic contact. The XRD patterns of the M-cell show the polycrystalline anatase TiO_2 phases. Other phases, such as Cu_2O and Cu, are hardly traced in the samples, which has some detrimental effects on photoelectrocatalytic (PEC) property of the heterostructure. The cross-sectional TEM micrograph reveals the characteristic feature of the sputtered TiO_2 top-layer, which is reportedly beneficial to the PEC activity. The cyclic voltammograms of two sample electrodes reveal that the M-cell is characterized by a rapid increase in the current density of about 0.27 mA cm^{-2} at 0.3 V vs. SCE, as compared with the bare TiO_2 electrode for a saturated current density of about 0.20 mA cm^{-2} at 0.0 V vs. SCE. This is ascribed to a better alignment of the flat bend potential between the oxide layers of the M-cell. Herein, the hydrogen yield rate at an applied bias of 1.0 V vs. SCE by the M-cell is 5.5, 2.1 and 4.2 μmol cm^{-2} h^{-1} under ultraviolet (UV), visible-light, and solar irradiation, respectively. The bare TiO_2 electrode evolves a hydrogen yield rate of 0.85 μmol cm^{-2} h^{-1} under UV irradiation and shows only a trace (<0.05 μmol cm^{-2} h^{-1}) of hydrogen evolution under visible-light irradiation. These are attributable to the additional bias for water splitting provided by the p-n CuO/ITO layer in the M-cell electrode.

Keywords: photoelectrode; CuO; solar light; water splitting

1 INTRODUCTION

Hydrogen is considered to be an environmental friendly and renewable energy source. The photocatalytic splitting water for hydrogen and oxygen evolution using solar light is a potentially clean and renewable source in the future. In principle, the efficiency of photoelectrochemical (PEC) conversion of solar energy is largely determined by the amount of the solar spectra absorbed by the photoelectrodes. The selection of specific semiconductor materials for PEC hydrogen production is difficult due to the necessity of simultaneously optimizing such very important features of semiconductor band gap, flat band potential, overpotential, and stability to corrosion. Only wide-band-gap oxides, such as titanium dioxide (TiO_2) and tungsten oxide (WO_3), are the ones that have a conduction-band potential sufficiently negative for the spontaneous hydrogen evolution from water. Thus, there has been extensive investigation on various application of TiO_2 since the discovery of the PEC water splitting on a TiO_2 electrode for hydrogen by Fujishima et al. 1972 [1]. Titania has various merits, such as favorable optical and electronic properties, low cost, chemical stability and non-toxicity [2]. However, the widespread technological use of TiO_2 is hindered by its low utilization of abundant solar energy in the visible-light region due to its wide band gap (3.0-3.2 eV). To extend its photocatalytic activities into the visible-light region, various approaches have been employed by coupling semiconductors with smaller band gaps, such as CdS, CdSe and CuO [3-5], and by doping with anionic, i.e., N, C and S, and/or cationic impurities in the past several decades [6,7]. For instance, TiO_2/ITO substrate coupled with CdS/CdSe top-layers has exhibited a significantly high hydrogen yield rate of 200.8 μmol cm^{-2} h^{-1} in a solution containing 0.35 M Na_2SO_3 and 0.24 M Na_2S under illumination of UV-cutoff AM 1.5 (100 mW cm^{-2}) [4]. However, the hydrogen evolution rate decreases slightly with operation time (~10%), due to the photocorrosion of the electrode. This implies that semiconductors with smaller band gaps, such as InP (1.5 eV), CdS (2.25 eV) and CdSe (1.7 eV), are not suitable candidates as the topmost layer in contact with the water/electrolyte. In other word, TiO_2 is still one of the most promising catalysts for water splitting application with good stability [8].

A photoelectrode that is connected directly in series with a photovoltaic cell (PV) to supply the extra needed bias voltage has been proposed to reduce, at least, or eliminate the necessity of applying external energy to the photoelectrolysis cell [9]. This configuration is known as an n-type photoanode-photovoltaic cell or p-type photocathode-photovoltaic Cell, namely, n-PV or p-PV cell. In the n-PV cell, majority carriers generated in the PV cell reduce protons in solution on a metal cathode and minority holes generated in the photoanode oxidize water at its

[1] Corresponding author: Tel.: +886-73617141ext.3218; fax: +886-75716013.
E-mail address: krwu@mail.nkmu.edu.tw (K.R. Wu).

surface. An n-PV junction can deliver an ideal solar-to-hydrogen conversion efficiency of 27% under optimal conditions, such as balanced photocurrent, proper ohmic contact, high light harvesting and low internal resistivity in the two electrodes [9]. Proper selection of the semiconductor photoelectrode characteristics is a crucial role to ensure that the energy necessary for water photoelectrolysis is gathered entirely from the solar light. Morisaki et al. firstly reported a hybrid TiO_2 photoanode coupled with a p-n junction Si photovoltaic device, by depositing the TiO_2 photoelectrode on top of the PV cell [10]. Light that was not absorbed by TiO_2 could be captured by the p-n Si photovoltaic layer, and thus provided the additional bias needed for water splitting. Several frameworks related to the use of a photoelectrode coupled to a PV layer have been reported in the past couple decades. For instance, Grätzel et al. reported a structured WO_3 and photoanode in series with a dye-sensitized TiO_2 solar cell with a solar-to-hydrogen efficiency of as high as 1.36% [11]. Miller et al. reported a single band gap device that used nanostructured WO_3, Fe_2O_3, or TiO_2 film photoanode coupled to a PV layer resulting to a solar-to-hydrogen efficiency of 0.6% with good stability [12,13]. On the other hand, a very efficient p-PV cell based on a p-$GaInP_2$ photocathode connected in series to a p-n GaAs junction photovoltaic layer has delivered a solar-to-hydrogen efficiency of 12.4% [14]. This configuration, however, shows a short lifetime of p-type photocathode and limited large-scale feasibility due to the expensive vapor-phase processing.

As one of the most popular p-type semiconductors, CuO is a monoclinic crystal structure with a narrow band gap of 1.2-1.5 eV. CuO is typically an opaque and more conductive material with a resistivity of 0.01-1 Ω cm [15]. Copper oxides are abundant, low-cost and non-toxic which make these oxides good candidates as the anode for lithium-ion batteries [16], diodes [17] and catalysts [18]. Although monocline CuO has a narrow band gap, it shows a quite narrow light-harvesting range; the UV adsorption behavior is relatively low. This makes a limited usage of CuO alone in solar-driven PEC applications, but heterostructured CuO/SnO_2 [19], CuO/TiO_2 [5] and CuO/ZnO [20] was used for capacitor, photocatalyst and solar energy conversion application. Meanwhile, reactive magnetron sputtering technique has been widely utilized for obtaining large-area uniform film and controlled thickness of various film oxides with well-controlled stoichiometry [15,21].

In this study, an n-PV cell (TiO_2/Ni/CuO/ITO) consisting of a TiO_2 film photoanode coupled to a p-n CuO/ITO layer was fabricated by using multi-target magnetron sputtering system and was investigated its PEC activity for solar-driven water splitting for hydrogen evolution.

2 EXPERIMENTAL PROCEDURE

The TiO_2/Ni/CuO/ITO multi-layered cells (M-cell) were deposited on commercial ITO (17 Ω/sq. and 100±10 nm thick, ShinAn SNP, Taiwan) substrates by radio frequency (rf) and direct current (DC) magnetron sputtering of a Cu, Ni and Ti targets (99.5% purity), respectively, using a multi-target sputtering system (Psur-100HB, Taiwan). Prior to deposition of the sample films, all ITO substrates were ultrasonically cleaned in an acetone bath and rinsed with distilled water and pre-sputtering process was applied for 10 min to clean the target surfaces for removing any possible contamination. The base pressure was set to $2.7x10^{-3}$ Pa, whereas the sputtering pressure of 0.8 Pa and 0.4 Pa were maintained as the reactive argon/oxygen mixture of 55/5 sccm and 50/10 was introduced, respectively, during the CuO and TiO_2 layer deposition of the M-cell. The ultra thin Ni layer was prepared without introducing O_2. The substrates were fixed in a disc fixture and rotated with a speed of 4 rpm in order to ensure film uniformity. The targets to the substrate distance were fixed at 60 mm and the substrate temperature was kept at 400°C for all sample depositions. Bare TiO_2 and CuO electrodes were also prepared on ITO substrates under the same sputtering conditions as the individual TiO_2 and CuO layer of the M-cell, respectively, but with longer deposition durations for comparison.

The crystal structures of the samples were analyzed using a high resolution X-ray diffractometer (XRD, Rigaku ATX-E) operating with Cu Kα radiation of 1.541 Å and a scan rate of $0.04^o/2\theta$ from $2\theta=20^o$ to 60^o. The surface morphology of the films was investigated by a scanning electron microscope (SEM, JEOL JSM-6700F). The microstructure was observed by a transmission electron microscope (TEM, Philips Tecnai 20) with a fully digitalized imaging system. A UV spectrophotometer (Hitachi UV-2900) was used to measure light transmittance of the samples with respect to the ambient air.

The photoelectrochemical properties of the samples were conducted in a standard three-electrode photochemical reactor, where a sample film anode with a size of 10 cm^2 was wired to a Pt foil cathode with a size of 16 cm^2 in a 4.0 N Na_2CO_3 solution (pH~11). A saturated calomel electrode (SCE) was set as a reference electrode. A potentiostat (CHI 610C, CH Instruments, Inc.) was used for photocurrent measurements using a scan rate of 5 mV s^{-1}, both in the darkness and under illumination. The Na_2CO_3 solution was purged with pure nitrogen for 10 min for removing dissolved oxygen in the solution before the tests and was continuously stirred with a magnetic stirrer during the tests. Three types of light sources, i.e., UV lamps (UV365, λ=365 nm), solar simulator (150 W, Newport, USA) and blue-light-emitting diodes (BLED, $420<\lambda<530$ nm centered at 470 nm), were chosen to provide irradiated light intensities of 2.7, 75.0 and 12.5 mW cm^{-2}, respectively. All of the chemicals were of analytical grade and the electrolyte was prepared with deionized distilled water. Hydrogen yield rates were determined by analyzing the gas that was liberated over the Pt foil cathode using gas chromatography (GC/TCD, HP4890).

3 RESULTS AND DISCUSSION

3.1 Microstructural and Optical Properties

One can see that the XRD patterns for the M-cell shows diffractional peaks at about 2θ= 32.3°, 35.6° and 38.6° that could be assigned to the crystalline CuO phase (JCPDS 80-0076) along with a preferential peak at 2θ=25.3° and a weak one at 2θ=48.0° of the anatase TiO_2 phase, as shown in Fig. 1. Other crystalline form of copper oxide, i.e., Cu_2O or Cu is hardly traced in sample M-cell, which has detrimental effect on photoelectrocatalytic property of the sample [22]. The UV-Vis absorption spectra of the M-cell and the bare TiO_2 and CuO electrodes are shown in Fig. 2. The absorption edges of the M-cell and bare CuO electrodes expectedly appear at larger wavelength than 800 nm with similar absorbance at the excitonic peaks, as compared with that of the bare TiO_2 at about 380 nm. The light absorption in the visible-light region of the M-cell electrode is highly enhanced by inclusion of the light-harvesting CuO layer. Thus, the M-cell electrode can harvest mostly the visible-light incidence of the solar light. However, the absorbance of the M-cell is lower than that of the bare CuO. This is possibly the effect of a thinner CuO layer in the M-cell electrode.

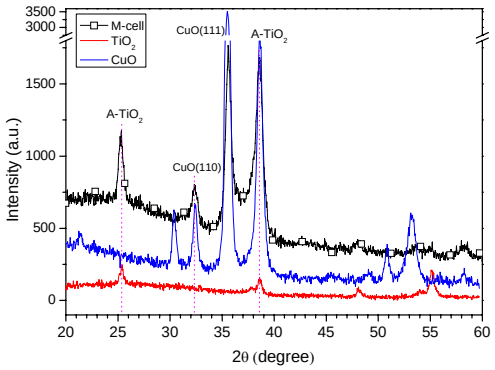

Fig. 1: XRD patterns of the M-cell electrode along with the bare TiO_2 and CuO films.

Figure 3 presents representative SEM morphologies of the M-cell and bare TiO_2 electrodes. Two samples exhibit quite different morphologies. The former has round-shaped particles lying on the nanoporous surface (Fig. 3a), while the latter shows a typical pyramidal shape of the DC-sputtered anatase TiO_2 phase with smaller particle sizes (Fig. 3b) [23] on the surface of typical polygon anatase TiO_2 particles consisting of the nanoporous surface. The cross-sectional TEM micrograph, depicted in Fig. 4, reveals the inherently columnar porous structure of the DC-sputtered TiO_2 top-layer which is reportedly benefits the light collection [23,24]. The photocatalytic activity could be enhanced [23]. Meantime, a typical amorphous TiO_2 zone was hardly found on the ultra thin Ni sub-layer by this successive magnetron sputtering technique [25]. The amorphous TiO_2 zones, inevitably formed above the inert substrates or a third phase likely produced at the heterostructured interface produced by two-step sputtering, reportedly inhibits PC activity [25]. Moreover, it has been pointed out that a back-to-back wireless configuration has the potential to be incorporated into a low-cost, applicable device structure [9]. The thicknesses of the TiO_2 top-layer and CuO light-absorbing layer are around 160 and 450 nm, respectively, whereas the ohmic Ni layer is quite indistinct from other layers with a thickness of ~10 nm in Fig. 4. The thicknesses of the bare TiO_2 and CuO electrodes are 560 and 620 nm, respectively, estimated by the cross-sectional SEM images (figures not shown here).

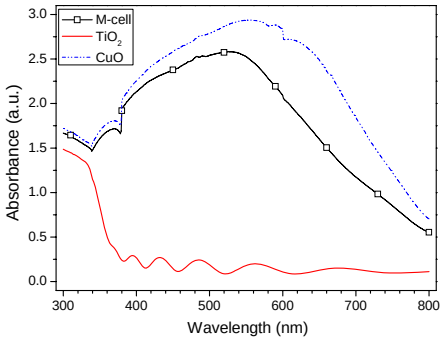

Fig. 2: UV-Vis absorption spectra of the M-cell, bare TiO_2 and CuO electrodes

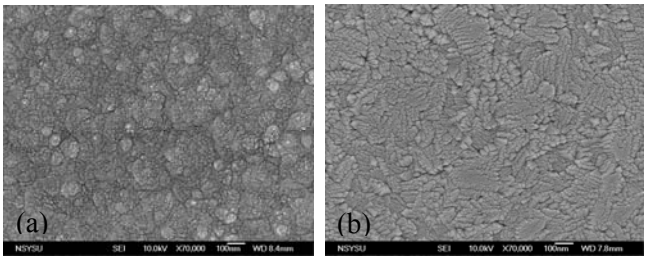

Fig. 3: SEM morphological views of (a) M-cell and (b) bare TiO_2 electrodes.

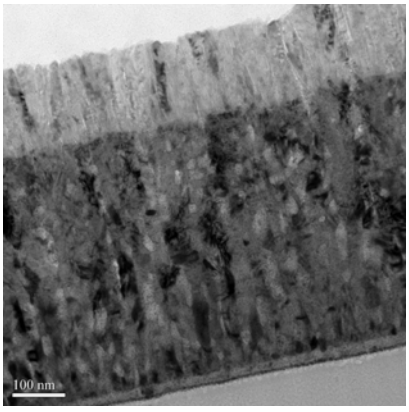

Fig. 4: Cross-sectional TEM micrograph of the M-cell electrode.

3.2 Photoelectrochemical Activities

Figure 5 shows the cyclic voltammograms of two sample electrodes under simulated solar illumination and darkness. The current response of M-cell electrode is faster

CTSI-Cleantech 2013, www.ct-si.org, ISBN 978-1-4822-0594-7

than that of the bare TiO_2 electrode under darkness, indicating that the M-cell electrode has a band edge structure with the lower resistance for superior charge transfer as a result of, in part, low resistance of both ITO and CuO semiconductors [3]. This also implies that an aligned conduction band edge was constructed in the M-cell electrode. Conversely, the bare TiO_2 electrode has a relatively high resistance, rendering a relatively high loss of charge transfer. Under simulated solar illumination, the M-cell is characterized by a rapid increase in the current density of about 0.27 mA cm^{-2} at 0.3 V vs. SCE, as compared with the sputtered bare TiO_2 electrode for a saturated current density of about 0.20 mA cm^{-2} at 0.0 V vs. SCE. These results suggest that the p-n CuO/ITO layer can significantly enhance the ability in the water splitting to produce hydrogen under solar/UV irradiation. Herein, the hydrogen yield rate at an applied bias of 1.0 V vs. SCE by sample M-cell is 5.5, 2.1 and 4.2 μmol cm^{-2} h^{-1} under UV365, BLED and solar irradiation, respectively. The bare TiO_2 electrode yielded a hydrogen yield rate of 0.85 μmol cm^{-2} h^{-1} under UV365 irradiation and shows only a trace (<0.05 μmol cm^{-2} h^{-1}) of hydrogen evolution under BLED irradiation. This is attributable to the additional bias for water splitting provided by the p-n CuO/ITO layer in the M-cell electrode. Nevertheless, the photocurrent of the M-cell is still low, due to partially insufficient thickness (~ 110 nm) of the ITO substrate and the light intensities applied. This will be further under investigation in our lab.

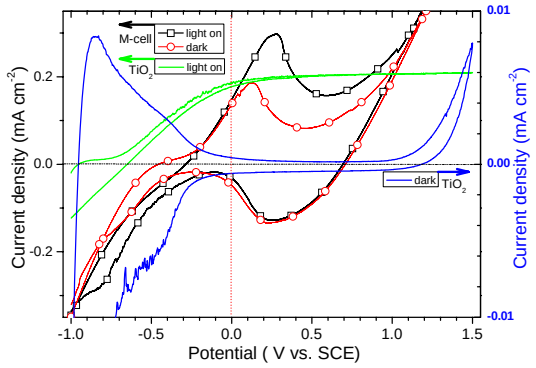

Fig. 5: Cyclic voltammograms of M-cell and bare TiO_2/ITO electrodes under solar illumination and darkness.

4. CONCLUSION

An M-cell (TiO_2/Ni/CuO/ITO) that is connected directly in series to supply the extra needed bias voltage was prepared in a single batch using a multi-target sputtering technique. The M-cell electrode shows a superior current response under darkness, indicating a better aligned band edge structure for a low resistance for charge transfer. The M-cell electrode exhibits the PEC ability of water spitting for hydrogen evolution under visible-light irradiation. This is ascribed to the additional bias for water splitting provided by the p-n CuO/ITO layer in the M-cell electrode.

Acknowledgements

The authors would like to thank the National Science Council of Taiwan, ROC, for financially supporting this research under Contract No. NSC 101-2221-E-022-007.

REFERENCES

[1] A. Fujishima, K. Honda, Nature 238 (1972) 37.
[2] A. Fujishima, T.N. Rao, D.A. Tryk, J. of Photochem. Photobiol. C 1 (2000) 1.
[3] Y.L. Lee, C.F. Chi, S.Y. Liau, Chem. Materials 22(3) (2010) 922.
[4] C.F. Chi, S.Y. Liau, Y.L. Lee, Nanotechnology 21 (2010) 025202.
[5] M.S. Hassan, T. Amna, H.Y. Kim, M.S. Khil, Composites B 45 (2013) 904.
[6] R. Asahi, T. Morikawa, T. Ohwaki, K. Aoki, Y. Taga, Science 293 (2001) 269.
[7] S.U.M. Khan, M. Al-Shahry, W. B. Ingler Jr., Science 297 (2002) 2243.
[8] T. Bak, J. Nowotny, M. Rekas, C.C. Sorrell, Intl. J. Hydrogen Energy 27 (2002) 991.
[9] M.G. Walter, E.L. Warren, J.R. McKone, S.W. Boettcher, Q. Mi, E.A. Santori, N.S. Lewis, Chem. Rev 110 (2010) 6446.
[10] H. Morisaki, T. Watanabe, M. Iwase, K. Yazawa, Appl. Phys. Lett. 29 (1976) 338.
[11] J. Brillet, M. Cornuz, F. Le Formal, J. H. Yum, M. Grätzel, K. Sivula, J. Mater. Res. 25 (2010) 17.
[12] E.L. Miller, B. Marsen, D. Paluselli, R. Rocheleau, Electrochem. Solid-State Lett. 8 (2005) A247.
[13] E.L. Miller, D. Paluselli, B. Marsen, R.E. Rocheleau, Sol. Energy Mater. Sol. Cells 88 (2005) 131.
[14] O. Khaselev, J.A. Turner, Science 280 (1998) 425.
[15] F.M. Li, R. Waddingham, W.I. Milne, A J. Flewitt, S. Speakman, J. Dutson, S. Wakeham, M. Thwaites, Thin Solid Films 520 (2011) 1278.
[16] J.Y. Xiang, J. P. Tu, L. Zhang, Y. Zhou, X. L. Wang, S.J. Shi, J. Power Sources 195 (2010) 313.
[17] İbrahim Y. Erdoğan, Ö. Güllü, J. Alloys and Compounds 492 (2010) 378.
[18] J.A. Switzer, H. M. Kothari, P. Poizot, S. Nakanishi, E.W. Bohannan, Nature 425 (2003) 490.
[19] M. Jayalakshmi, K. Balasubramanian, Int. J. Electrochem. Sci. 4 (2009) 571.
[20] S. Jung, S. Jeon, K. Yong, Nanotechnology 22 (2011) 015606.
[21] K. Akimoto, S. Ishizuka, M. Yanagita, Y. Nawa, Goutam K. Paul, T. Sakurai, Sol. Energy 80 (2006) 715.
[22] L. Huang, F. Peng, H. Yu, H. Wang, Solid State Sci. 11 (2009) 129.
[23] K.R. Wu, C.H. Hung, M.H. Tsai, Appl. Catal. B: Environ. 92 (2009) 357.
[24] J. Rodríguez, M. Gómez, S.-E. Lindquist, C. G. Granqvist, Thin Solid Films 360 (2000) 250.
[25] O. Zywitzki, T. Modes, H. Sahm, P. Frach, K. Goedicke, D. Glöβ, Surf. Coat. Technol. 180-181 (2004) 538.